Electrostatic Multilayer Deposition of a Gold−Dendrimer Nanocomposite

Jin-An He, Regina Valluzzi, Ke Yang, Tigran Dolukhanyan, Changmo Sung, Jayant Kumar, and Sukant K. Tripathy*

Center for Advanced Materials, University of Massachusetts-Lowell, Lowell, Massachusetts 01854

Lynne Samuelson

Materials Science Team, U.S. Army Soldier & Biological Chemical Command, Soldier Systems Center, Natick, Massachusetts 01760

Lajos Balogh and Donald A. Tomalia

Michigan Molecular Institute, 1910 West Saint Andrews Road, Midland, Michigan 48640

Received May 27, 1999. Revised Manuscript Received September 27, 1999

Poly(amidoamine) (PAMAM) dendrimers can be used as a polymeric template/stabilizer/reservoir to prepare stable gold−dendrimer nanocomposites by reducing PAMAM−tetrachloroaurate polysalts using hydrazine. In the gold−dendrimer nanocomposite, the presence of elemental gold is indicated by its characteristic plasmon absorption peak at 529 nm in aqueous solution and is visualized by transmission electron microscopy (TEM) equipped with energy-dispersive X-ray spectroscopy (EDXS). Electrostatic layer-by-layer assembly of the gold−dendrimer nanocomposite using poly(sodium 4-styrenesulfonate) (PSS) as the oppositely charged polyelectrolyte leading to nanoscale uniform multilayers of gold−dendrimer nanoclusters is reported. UV−vis absorption spectra from the consecutive multilayers indicated that each bilayer growth is regular, even though a 20 nm absorption bathochromic shift takes place in the film. TEM of PSS/gold−dendrimer nanocomposite film demonstrates that gold nanoparticles (5−20 nm) appear as aggregates within a gold−dendrimer nanocomposite monolayer, an observation borne out by crystalline gold electron diffraction patterns obtained from PSS/gold−dendrimer nanocomposite. Atomic force microscopy (AFM) of PSS/gold−dendrimer nanocomposite film indicates that the nanoclusters are arrayed with high uniformity at the nanometer scale.

Introduction

Nanostructured clusters of semiconductors and metals, which differ from the bulk material due to surface, shape, and quantum size effects, have been designed to possess unique properties due to electron confinement.[1] The unique properties of nanosized metal particles can be utilized in a broad range of fields, from catalysis to nonlinear optical devices.[2] Gold is a particularly interesting metal to study because of its well-defined electronic and aggregate structures and its optical and biological applications, among others.[3] For example, it has been extensively studied in areas such as a base layer for self-assembled monolayers and as a nonlinear optical material embedded in silica glass, where it shows a large third-order optical nonlinearity with a magnitude of 1.2×10^{-7} esu.[4] A number of different approaches have been developed to prepare various metal nanoparticles.[5] Some of these methods include photoreduction and reduction using different reducing agents in association with protective polymers or surfactants to avoid agglomeration.[6] Metallic gold is usually produced by chemical reductions using sodium citrate, citric acid, hydrazine, and hydrogen or electrochemical deposition, and the color is the function of the size and shape of the metal.[7] Subsequently, various techniques for film formation have been used to obtain ordered nanoparticles assemblies, including Langmuir−Blodgett and electrostatic adsorption methods.[8]

Electrostatic layer-by-layer (LBL) deposition of oppositely charged polyelectrolytes[9] and other species such

* To whom correspondence should be addressed.

(1) (a) Siegel, R. *Nanostruct. Mater.* **1993**, *3*, 1. (b) Ayappan, S.; Gopalan, R. S.; Subbana, G. N.; Rao, C. N. R. *J. Mater. Res.* **1997**, *12*, 398.

(2) (a) Henglein, A.; Lillie, J. *J. Phys. Chem.* **1981**, *85*, 1246. (b) Suzuki, M.; Taga, Y. *J. Appl. Phys.* **1992**, *71*, 2848. (c) Puech, K.; Blau, W.; Grund, A.; Bubeck, C.; Cardenas, G. *Opt. Lett.* **1995**, *20*, 1613.

(3) Colvin, V. L.; Goldstein, A. N.; Alivisatos, A. P. *J. Am. Chem. Soc.* **1992**, *114*, 5221.

(4) Fukumi, K.; Chayahara, A.; Kadono, K.; et al. *Jpn. J. Appl. Phys.* **1991**, *30*, L742.

(5) (a) Huang, H. H.; Yan, F. Q.; Kek, Y. M.; Chew, C. H.; Xu, G. Q.; Ji, W.; Oh, P. S.; Tang, S. H. *Langmuir* **1997**, *13*, 172. (b) Brugger, P. A.; Guendet, P.; Gratzel, M. *J. Am. Chem. Soc.* **1981**, *103*, 2923.

(6) (a) Huang, H. H.; Ni, X. P.; Loy, G. L.; Tan, K. L.; Loh, F. C.; Deng, J. F.; Xu, G. Q. *Langmuir* **1996**, *12*, 909. (b) Weller, H. *Angew. Chem., Int. Ed. Engl.* **1996**, *35*, 1079.

(7) Martin, C. R. *Science* **1994**, *266*, 1961.

(8) Fendler, J. H. *Chem. Mater.* **1996**, *8*, 1616.

10.1021/cm990311c CCC: $18.00
Published on Web 10/27/1999

as proteins,[10] DNA,[11] conducting polymers,[12] zirconium phosphate,[13] dyes,[14] and metal or semiconductive nanoparticles[15] is of pressing interest as a facile means of creating ordered, functionalized films. By using suitably charged polyions as counterions, oppositely charged materials of interest can be deposited to create ultrathin films with a range of structure and important electronic and optical properties.[16] In our group, acentric multilayers of azo polymers with novel optical properties have been investigated.[17] This approach has been further extended to grow acentric bilayers of a polyelectrolyte and nanostructured materials such as purple membrane fragments[18] and polydiacetylene microcrystals.[19]

Dendrimers are regularly branched macromolecules composed of multifunctional monomers.[20] Use of poly(amidoamine) (PAMAM) dendrimers as platforms for the deposition of gold colloid monolayers on various substrates indicated an unusual degree of control and uniformity.[21] Dendrimers are now recognized as monodispersed nanoreactors, possessing architectures that allow the preorganization of metal ions within their interiors.[22] PAMAM dendrimers are monomodal and have a well-defined size and shape. Therefore, PAMAM has been utilized as a nanoscale template/stabilizer/container in the synthesis and stabilization of inorganic clusters including zerovalent metal clusters by reaction of preorganized reactants in the dendrimer interior. Balogh and co-workers have reported the synthesis and characterization of transition-metal sulfide−dendrimer nanocomposites.[23,24] The formation and mechanism of metallic copper-containing PAMAM dendrimer nanocomposites with a variety of end groups were also discussed.[25] In the meantime, Zhao and Crooks have reported the synthesis of copper nanoclusters within a dendrimer through reduction in a mixing solution of $CuSO_4$ and G4-OH PAMAM dendrimer by $NaBH_4$.[26] Esumi and co-workers also obtain gold nanoparticles by reduction of metal salt with UV irradiation using dendrimers as stabilizer.[27] They conclude that the size of synthesized metal particles, which defines their electronic and optical properties, can be controlled by varying the chemical structure and size of the dendrimers.

In these well-defined dendrimers, a predetermined number of metal atoms are dispersed in the form of small domains to give a hybrid nanocomposite cluster. Moreover, these dendrimers possess nanometer-scale voids in their molecular skeleton,[28] which is suitable to confine metal nanoparticles in the interior of the dendrimers. This may efficiently prevent coalescence of the metal nanoparticles compared with other surfactants including poly(*N*-vinyl-2-pyrrolidone).[27] The methodology to synthesize extremely stable metal−dendrimer nanocomposites has recently been used to produce Pt- or Pd-containing dendrimer nanoclusters, which can be used as homogeneous catalysts for hydrogenation of alkenes. More interestingly, the authors found that the catalytic activities of the nanocomposites depend on the dendrimer generation used.[29]

Fabrication of ordered semiconducting and metallic nanoparticles on solid substrates has recently been a topic for substantial research due to their multifunctional electronic, optical, and catalytic properties.[30] Given the fascinating properties of metal−dendrimer nanomaterials,[25−29] it is important to explore a method to assemble these materials to form well-defined thin films. The surface charges of these dendrimer-based metal nanocomposites may be easily produced from the end groups of dendrimers by adjusting the pH of their solutions.[20] Thus, the electrostatic LBL self-assembly of these dendrimer-based metal nanocomposites can open up a shortcut to construct multilayers of polymer-protected nanoscale metals with a range of interesting optical and electronic properties.

In the present publication, nanostructured gold particles incorporated into dendrimers have been synthesized, and the nanosized nanocomposites have been deposited as a multilayer thin film using electrostatic LBL deposition techniques. The gold−dendrimer nanocomposites are stable in solution over time. The uniform size of the gold−dendrimer nanoclusters and the presence of gold cluster within the interior of the dendrimers are supported by their transmission electron microscopy (TEM) and atomic force microscopy (AFM) images. UV−vis absorption spectra indicate that high-optical-quality multilayers with stepwise growth of gold−dendrimer nanocomposites and poly(sodium 4-styrenesulfonate)

(9) (a) Lvov, Y.; Essler, F.; Decher, G. *J. Phys. Chem.* **1993**, *97*, 13773. (b) Lvov, Y.; Haas, H.; Decher, G.; Mohwald, H.; Kalachev, A. *J. Phys. Chem.* **1993**, *97*, 12835.

(10) (a) Lvov, Y.; Ariga, K.; Ichinose, I.; Kunitake, T. *J. Am. Chem. Soc.* **1995**, *117*, 6117. (b) Caruso, F.; Niikura, K.; Furlong, D. N.; Okahata, Y. *Langmuir* **1997**, *13*, 3427. (c) Onda, M.; Lvov, Y.; Ariga, K.; Kunitake, T. *Biotech. Bioeng.* **1996**, *51*, 163.

(11) Lvov, Y.; Decher, G.; Sukhorukov, G. *Macromolecules* **1993**, *26*, 5396.

(12) (a) Cheung, J. H.; Fou, A. F.; Rubner, M. F. *Thin Solid Films* **1994**, *244*, 985. (b) Cheung, J. H.; Stockton, W. B.; Rubner, M. F. *Macromolecules* **1997**, *30*, 2712.

(13) Fang, M. M.; Kaschak, D. M.; Sutorik, A. C.; Mallouk, T. E. *J. Am. Chem. Soc.* **1997**, *119*, 12184.

(14) Ariga, K.; Lvov, Y.; Kunitake, T. *J. Am. Chem. Soc.* **1997**, *119*, 2224.

(15) (a) Feldheim, D. L.; Crabar, K. C.; Natan, M. J.; Mallouk, T. E. *J. Am. Chem. Soc.* **1996**, *118*, 7640. (b) Schmitt, J.; Decher, G.; Dressik, W. J.; Branduo, S. L.; Geer, R. E.; Shashidhal, R.; Calvert, J. *Adv. Mater.* **1997**, *9*, 61.

(16) Decher, G. *Science* **1997**, *277*, 1232.

(17) (a) Wang, X. G.; Balasubramanian, S.; Li, L.; Jiang, X. L.; Sandman, D. J.; Rubner, M. F.; Kumar, J.; Tripathy, S. K. *Macromol. Rapid Commun.* **1997**, *18*, 451. (b) Balasubramanian, S.; Wang, X. G.; Wang, H. C.; Yang, K.; Li, L.; Kumar, J.; Tripathy, S. K. *Chem. Mater.* **1998**, *10*, 1554.

(18) He, J.-A.; Samuelson, L.; Li, L.; Kumar, J.; Tripathy, S. K. *Langmuir* **1998**, *14*, 1674.

(19) Tripathy, S. K.; Katagi, H.; Kasai, H.; Balasubramanian, S.; Oshikiri, H.; Kumar, J.; Oikawa, H.; Okada, S.; Nakanishi, H. *Jpn. J. Appl. Phys.* **1998**, *37*, L343.

(20) Tomalia, D. A.; Naylor, A. M.; Goddard, W. A. I. *Angew. Chem., Int. Ed. Engl.* **1990**, *29*, 138.

(21) (a) Bar, G.; Rubin, S.; Cutts, R. W.; Taylor, T. N.; Zawodinski, T. A. J. *Langmuir* **1996**, *12*, 1172. (b) Rubin, S.; Bar, G.; Taylor, T. N.; Cutts, R. W.; Zawodinski, T. A. J. *J. Vac. Sci. Technol. A* **1996**, *14*, 1870.

(22) Ottaviani, M. F.; Montalti, F.; Turro, N. J.; Tomalia, D. A. *J. Phys. Chem. B* **1997**, *101*, 158.

(23) Balogh, L.; Swanson, D. R.; Spindler, R.; Tomalia, D. A. *Polym. Mater. Sci. Eng.* **1997**, *77*, 118.

(24) Beck Tan, N.; Balogh, L.; Trevino, S. *Polym. Mater. Sci. Eng.* **1997**, *77*, 120.

(25) Balogh, L.; Tomalia, D. A. *J. Am. Chem. Soc.* **1998**, *120*, 7355.

(26) Zhao, M. Q.; Sun, L.; Crooks, R. M. *J. Am. Chem. Soc.* **1998**, *120*, 4877.

(27) Esumi, K.; Suzuki, A.; Aihara, N.; Usui, K.; Torigoe, K. *Langmuir* **1998**, *14*, 3157.

(28) Dagani, R. *Chem. Eng. News* **1999**, *Feb. 8*, 33

(29) Zhao, M. Q.; Crooks, R. M. *Angew. Chem., Int. Ed. Engl.* **1999**, *38*, 364.

(30) (a) Yonezawa, T.; Matsune, H.; Kunitake, T. *Chem. Mater.* **1999**, *11*, 33. (b) Shipway, A. N.; Lahav, M.; Blonder, R.; Willner, I. *Chem. Mater.* **1999**, *11*, 13 and references therein.

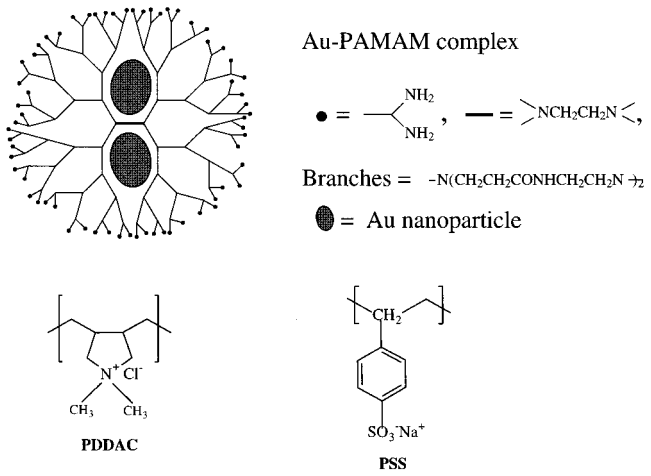

Figure 1. Structures of the polyelectrolytes and Au−dendrimer (G5 PAMAM) nanocomposite for electrostatic LBL assembly.

(PSS) are obtained using polyanionic PSS as an oppositely charged polyelectrolyte. The films obtained appear uniform in atomic force microscopy. The present assembly method for gold−dendrimer nanocomposite can be extended to immobilize other semiconductor- and metal-containing dendrimer nanocomposites, in which the relevant solution conditions and counter polyions can be selected depending on the end groups of the different dendrimers.

Materials and Method

Materials. Amino-terminated generation 5 (G5) PAMAM dendrimers based on an ethylenediamine core (PAMAM_E5·$NHCH_2CH_2NH_2$, M_n = 28 826) were obtained from Dendritech and used without further purification. Poly(dimethyl diallylammonium chloride) (PDAC, 20 wt % in water, molecular weight 200 000−350 000), poly(sodium 4-styrenesulfonate) (molecular weight 70 000), $HAuCl_4$, and $NaAuCl_4$ were purchased from Aldrich and were used as received.

Sample Preparation. Preparation of stable metallic gold−dendrimer nanocomposites were achieved in aqueous solution by mixing dilute (1 mM) aqueous solutions of $[AuCl_4]^-$ with the aqueous solution of the PAMAM dendrimer at a molar ratio of 10 gold atoms per dendrimer. The yellow $[AuCl_4]^-$ solution lost its yellow color immediately upon mixing with the PAMAM, indicating a change in the electronic environment of the tetrachloroaurate counterion; i.e., the $[AuCl_4]^-$ had been trapped into the interior of the PAMAM dendrimer, and the formation of a polysalt (PAMAM_E5·$NHCH_2CH_2NH_3^+$)$[AuCl_4]_{10}^-$ between the dendrimer nitrogens and the complex anion had occurred. Room temperature reduction of the tetrachloroaurate ions bound as counterions to the amino groups of the dendrimer surface and interior with a slight excess of hydrazine (50 mol % excess) resulted in deep red solutions without any Tyndall effect. Concentrations of the final nanocomposite solutions were 3.78 g/L for the dendrimer and 0.58 g/L for gold.

Layer-by-Layer Deposition. The chemical structures of Au−dendrimer (PAMAM G5) nanocomposite, PDAC, and PSS are shown in Figure 1. Polycationic PDAC and polyanionic PSS were dissolved in Milli-Q water at a concentration of 2.0 mg/mL, containing 0.5 M NaCl at a pH of 6.8 for the multilayer adsorption. All solid supports were pretreated for 30 min in an ultrasonic bath at 25 °C in a mixture of ethanol/acetone/chloroform (2/1/1, v/v/v) and then again in 2% KOH aqueous solution under the same conditions. After treatment, the slides were thoroughly rinsed with Milli-Q water and stored in Milli-Q water prior to use. The pretreatment procedure was used to partially hydrolyze the surface of the support substrate and render a net negative surface charge for subsequent polycation (PDAC) adsorption.

The fabrication procedure of the PSS/gold−dendrimer nanocomposite multilayers is schematically presented in Figure 2. Briefly, a negatively charged solid support is primed by adsorbing a layer of PDAC onto its surface (2 mg/mL PDAC, 5 min). The primed substrate is then immersed into a 2 mg/mL PSS solution for 5 min, and a layer of PSS with excess negative bound charge is adsorbed. The modified substrate is then rinsed with water and dried using nitrogen. It is subsequently immersed into a gold−dendrimer nanocomposite solution (pH 5.0, 0.58 g/L for gold) for 5 min, rinsed with water for 2 min and again dried using nitrogen. This process is repeated until the desired number of bilayers of PSS/gold−dendrimer complex is obtained.

Sample Characterization. UV−visible absorption spectra were obtained for the solutions of the nanocomposite and for the deposited films using a Perkin-Elmer Lambda-9 UV/vis/near-infrared spectrophotometer. The samples of the PSS/Au−dendrimer multilayer growth for UV−visible absorption measurements were deposited on the quartz slides. Bright-field TEM images were performed using a Philips EM400T (operating at 120 kV) equipped with Noran instrument energy-dispersive X-ray spectrometer (EDXS). AFM observations were performed with an atomic force microscope (Park Scientific, CA) operated in the contact mode using a standard silicon nitride cantilever (force constant 0.03 N/m, resonant frequency 15 Hz) in ambient air. The scan rate is 1 line/s, and the set point is 50 nN. The samples for AFM and TEM were prepared on silicon wafers and carbon-covered 200-mesh copper grids, respectively, by the electrostatic LBL deposition method described above.

Results and Discussion

Characterization of the Gold−Dendrimer Nanocomposite. The UV−visible absorption spectrum of the stable aqueous solution of zerovalent gold−PAMAM (G5) dendrimer nanocomposite is presented in Figure 3. The nanocomposite solution showed an absorption band at 529 nm, which is a characteristic resonance of elemental gold particles.[30a,31] The appearance of the plasmon resonance is also in accordance with the observation from the work of Esumi and co-workers who concluded that the band comes from the gold particles.[27] The position of the plasmon peak without obvious shift in comparison with other preparation methods indicates that the gold atoms are not covalently bonded to the dendrimers but are present as very small gold particles trapped inside the dendrimer. An aqueous solution of gold−dendrimer nanocomposites stored for over 180 days at room temperature remains stable and does not agglomerate. The solubility and stability of the nanocomposite solution are not measurably affected by the presence of these gold particles, perhaps due to the isolation of the gold particles in the interiors of the dendrimers; i.e., the Au−dendrimer nanocluster has an architecture similar to the dendrimer-encapsulated Cu, Pd, and Pt nanoparticles.[25,26,29]

Microscopy techniques, notably transmission electron microscopy and electron diffraction, have been used to characterize metal−dendrimer nanocomposites.[27,29] The one bilayer of PSS/gold−dendrimer nanocomposites deposited onto a carbon-covered copper grid by electrostatic LBL method was observed using TEM in order to visualize the configuration of individual gold−dendrimer nanocomposites. A bright-field TEM image of the PSS/gold−dendrimer nanocluster film is shown in Figure 4a. A number of small, spherelike dark spots with

(31) Doremus, R. H.; Rao, P. *J. Mater. Res.* **1996**, *11*, 2834.

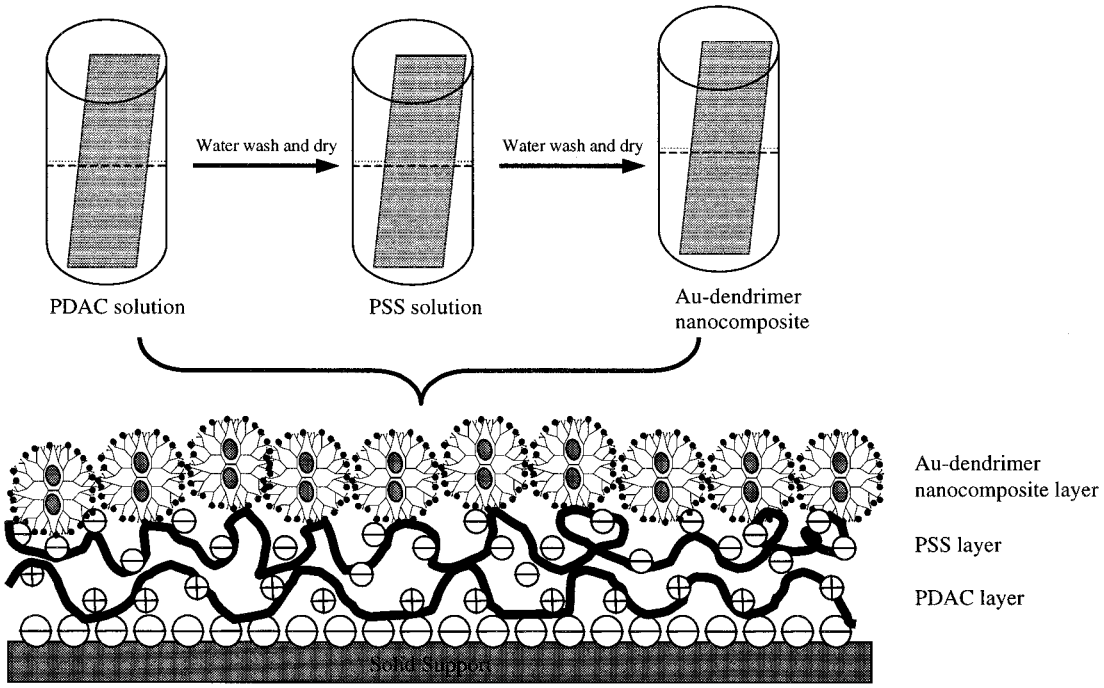

Figure 2. Schematic illustration of the procedure for fabrication of the PSS/Au−dendrimer nanocomposite film on the negatively charged substrate and the architecture of resulting film.

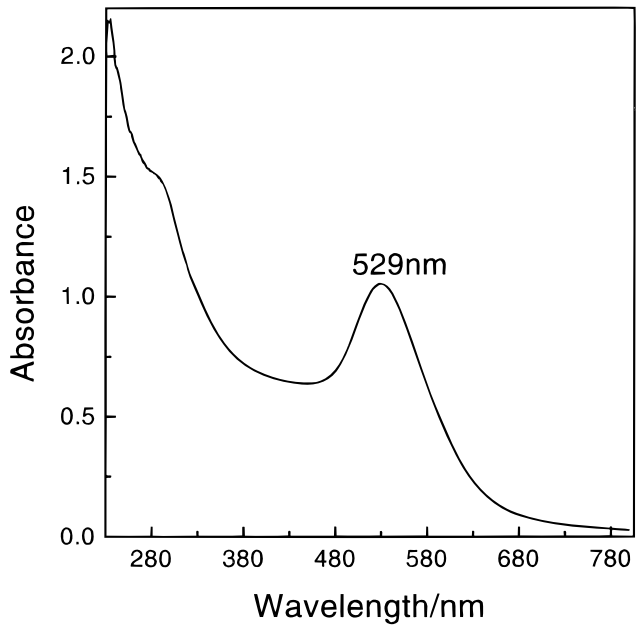

Figure 3. UV−vis absorption spectrum of Au−dendrimer (G5 PAMAM) nanocomposites in an aqueous solution.

size distribution from 5 to 20 nm can be clearly observed and are interpreted to be the aggregates of gold−PAMAM nanocomposite particles formed in the gold−dendrimer monolayer film. The elemental composition from the nanoparticle-rich domain was analyzed by EDXS, and the results are given in Figure 4b. From Figure 4b, the characteristic X-ray emission lines from Au element, which are M_α (2.12 keV), $L_{\alpha 1}$ (9.63 keV), and $L_{\beta 1}$ (11.44 keV), are observed. These results confirm that these dark nanoclusters are actually gold particles. The X-ray emissions of carbon (K, 0.277 keV) and nitrogen (K, 0.392keV) elements from PAMAM dendrimer cannot be distinguished from Figure 4b due to the interference of carbon from the carbon-covered copper grid. However, surface morphological investigation of the PSS/Au−dendrimer film by the AFM discussed later provides additional evidence that the PAMAM dendrimers exist in the nanocomposite film. The characteristic X-ray emission peaks of sulfur and oxygen located at 2.307 (K_α) and 0.525 (K) keV, respectively, are believed to come from the sulfonate group of poly(sodium 4-styrenesulfonate). The result shows that PSS is present in the composite film. The electrostatic attraction between PSS and the Au−dendrimer nanocluster is the dominant driving force for the film formation. The polycrystalline gold electron diffraction pattern from PSS/Au−dendrimer film is presented in Figure 4c. Crystalline features of Au particles were confirmed by fine discrete spot patterns overlapped with a ring pattern from carbon. A dark-field image of Au particles has not been successfully obtained due to very weak scattering from the nanostructured Au particles. The result further indicates the existence of gold clusters in the gold−dendrimer nanocomposite after hydrazine reduction. The appearance of Au−dendrimer nanocomposite by TEM is similar to the result from Pd− and Pt−dendrimer nanocomposites,[29] which verifies the inference that gold particles can be located inside the dendrimer. The architecture of Au−dendrimer nanocomposite would have little or no effect on properties such as solubility or solution stability of the dendrimer because the branches of the dendrimer would shield interactions between gold and the environment outside the dendrimer core. On the basis of the UV and TEM results of the gold−dendrimer nanocomposites, it is concluded that a stable intradendrimeric gold nanocomposite may be prepared using dendrimers as a template/stabilizer/reservoir through chemical reduction of metal ions within the dendrimer.

Fabrication of PSS/Gold−Dendrimer Nanocomposite Multilayers. Construction of controlled and homogeneous films of nanostructured materials is an

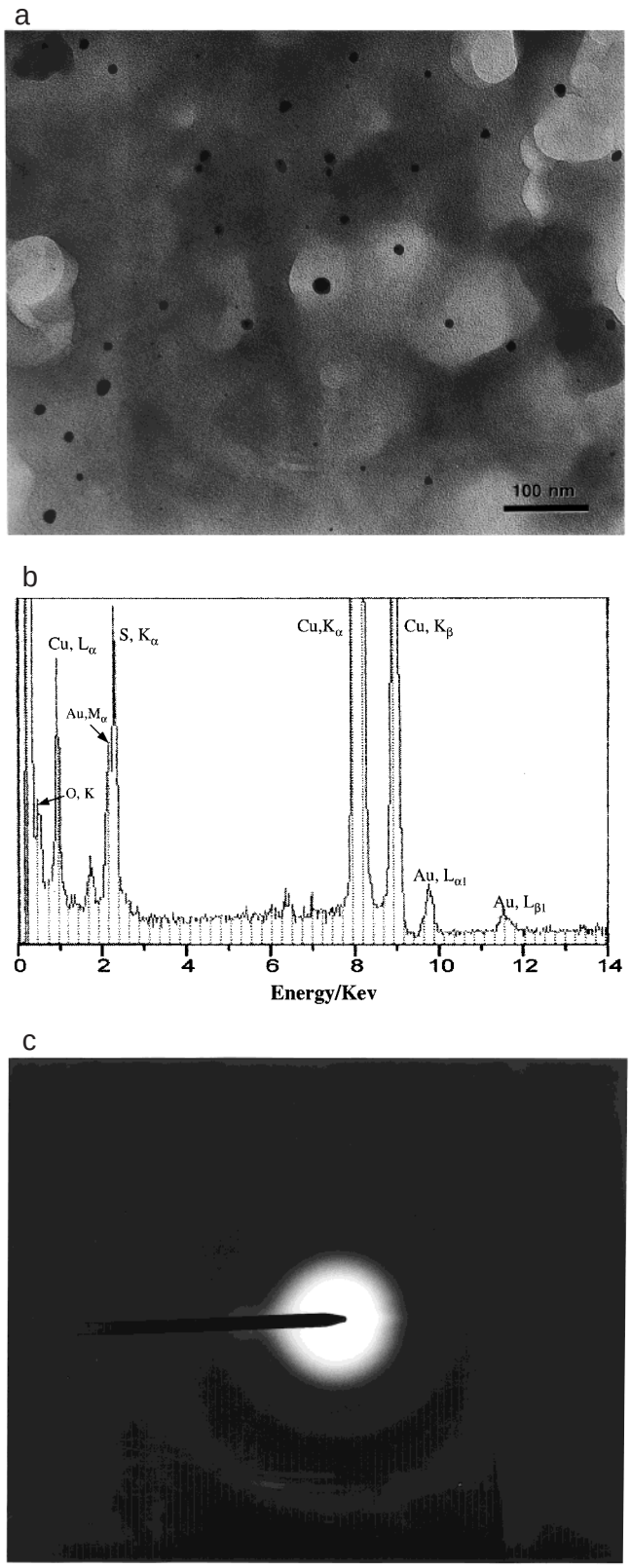

Figure 4. (a) Bright-field TEM image of PSS/Au−dendrimer nanocomposites deposited onto carbon-covered copper grid. (b) EDXS spectrum of the PSS/Au−dendrimer film, the X-ray emission lines of Cu from copper grid. (c) Electron diffraction pattern from the PSS/Au−dendrimer film.

important target of modern materials research.[8,32] Intradendrimer metal nanocomposites can be easily as-

(32) Schmid, G. *Chem. Rev.* **1992**, *92*, 1709.

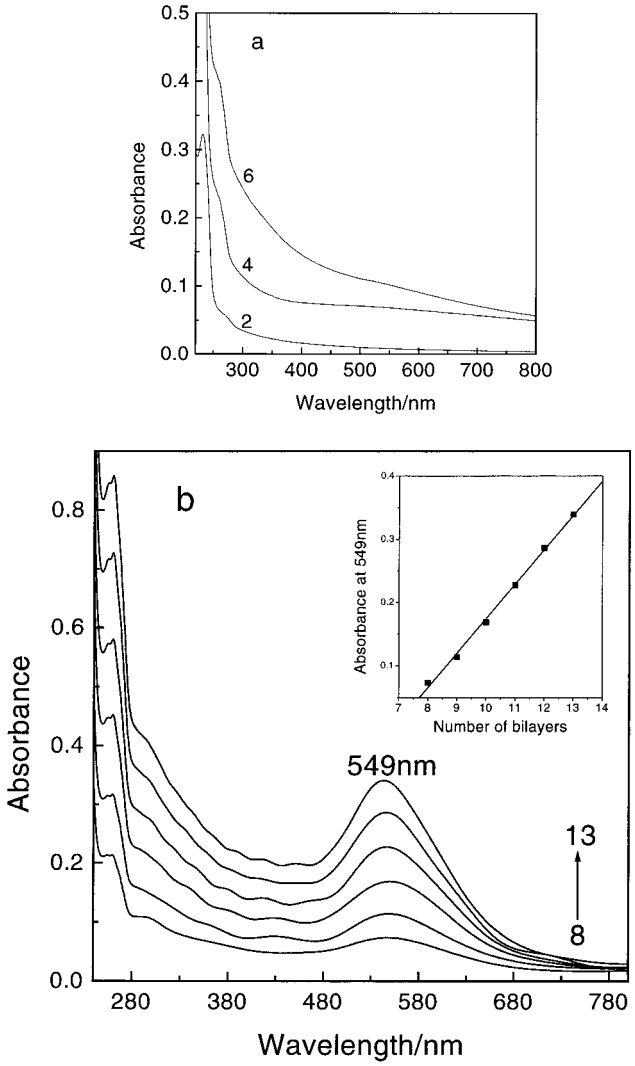

Figure 5. UV−vis absorption spectra of PSS/Au−dendrimer nanocomposite multilayers on a quartz slide. (a) Curves corresponding to adsorption of 2, 4, and 6 alternate PSS/Au−dendrimer bilayers. (b) Curves corresponding to adsorption of 8−13 PSS/Au−dendrimer complex bilayers. The inset shows the increases of absorbance at 549 nm with the number of bilayers.

sembled into supramolecular structures by electrostatic layer-by-layer deposition employing the well-controlled surface chemistry of dendrimers. The well-defined, multiply charged surface of the gold−dendrimer nanocomposite, due to the terminal amino groups of the dendrimer, is utilized for the multilayer assembly. The nanocomposite has been deposited onto the negatively charged sulfonated polystyrene (PSS) film surface and a uniform multilayer of PSS/gold−dendrimer nanocomposite has been obtained. Figure 5 presents the UV−vis spectra of the PSS/gold−dendrimer nanocomposite multilayers. From Figure 5a, we can see that the absorbance in the UV region increases with the increase of the number of bilayers, but the plasmon peak at 529 nm characteristic of gold particle in the solution does not appear until six adsorption cycles. The result does indicate that the gold−dendrimer nanocomposite could be adsorbed onto the PSS film at this stage because there exists the absorbance increase in the UV range, and a golden hue can obviously be seen by the naked eye from the stepwise growth of the PSS/Au−dendrimer

multilayers on solid support. A uniform array of the Au−dendrimer nanocomposite on the PSS layer is further confirmed from AFM studies. A possible explanation for the absence of the plasmon resonance from the spectra of the gold particles in the early stage of the deposition is that the ultrathin film (fewer than eight bilayers) of the PSS/gold−dendrimer nanocomposite structure is extremely smooth and acts like a gold mirror, reflecting the incident light. This reflection appears as a background absorption in the spectrophotometer and masks the plasmon absorption peak. Upon further repetition of the dipping cycle, both the thickness and the surface roughness of the film increase, and the reflection and the mirroring effect perhaps is eventually lost after the deposition of eight bilayers. Therefore, the spectral mask effect due to the reflection of the gold mirror vanishes, which results in the appearance of the characteristic plasmon peak of the gold particles in a thicker PSS/Au−dendrimer nanocomposite film.

The spectroscopic investigations presented in Figure 5b verify our above assumption. Figure 5b is a series of UV−vis absorption spectra of the PSS/gold−dendrimer nanocomposite multilayers when the number of the bilayers is greater than eight (including eight bilayers). As shown, an absorption band appears at 549 nm, and its absorbance linearly increases with the increase of the number of bilayers shown in the inset. This maximum absorbance at 549 nm should originate from the gold nanoparticles, even though it has a 20 nm redshift in comparison with that of the solution. The reason for this redshift perhaps comes from two factors. One is that, due to the size increase of gold particles, the plasmon band shifts to longer wavelengths.[27,31] Another is the enormous change of electronic (dielectric) environment of gold−dendrimer nanocomposites when immobilized by electrostatic interaction between PSS and the amino-terminated PAMAM dendrimer. In the present system, the first reason may be ruled out due to the configuration of Au−dendrimer nanocomposite. The further coalescence of gold particles after formation of the PSS/Au−dendrimer multilayers does not seem possible because the gold particles had been effectively protected by their location in the interior voids of the PAMAM dendrimers. On the other hand, the electrostatic interaction between the amino groups of the dendrimer and the sulfonate groups of PSS molecules, which leads to the formation of PSS/gold−dendrimer nanocomposite multilayers, should result in a change in the polarizing medium and hence the electronic property of gold domains being incorporated into the dendrimer. The change of dielectric environment of gold particles results in the absorption redshift of the Au−dendrimer nanocomposite in the film.

The proportionate increase of the absorbance at 549 nm with the number of bilayer strongly indicates that the electrostatic layer-by-layer deposition for the PSS/gold−dendrimer composite multilayer is a linear process and that each layer of growth contributes the same amount of gold−dendrimer nanocomposites to the film assembly. Use of gold−dendrimer nanocomposites offers unprecedented control of multilayer formation because the chemistry, shape, and size of the dendrimers used determines the morphology of the fabricated films.

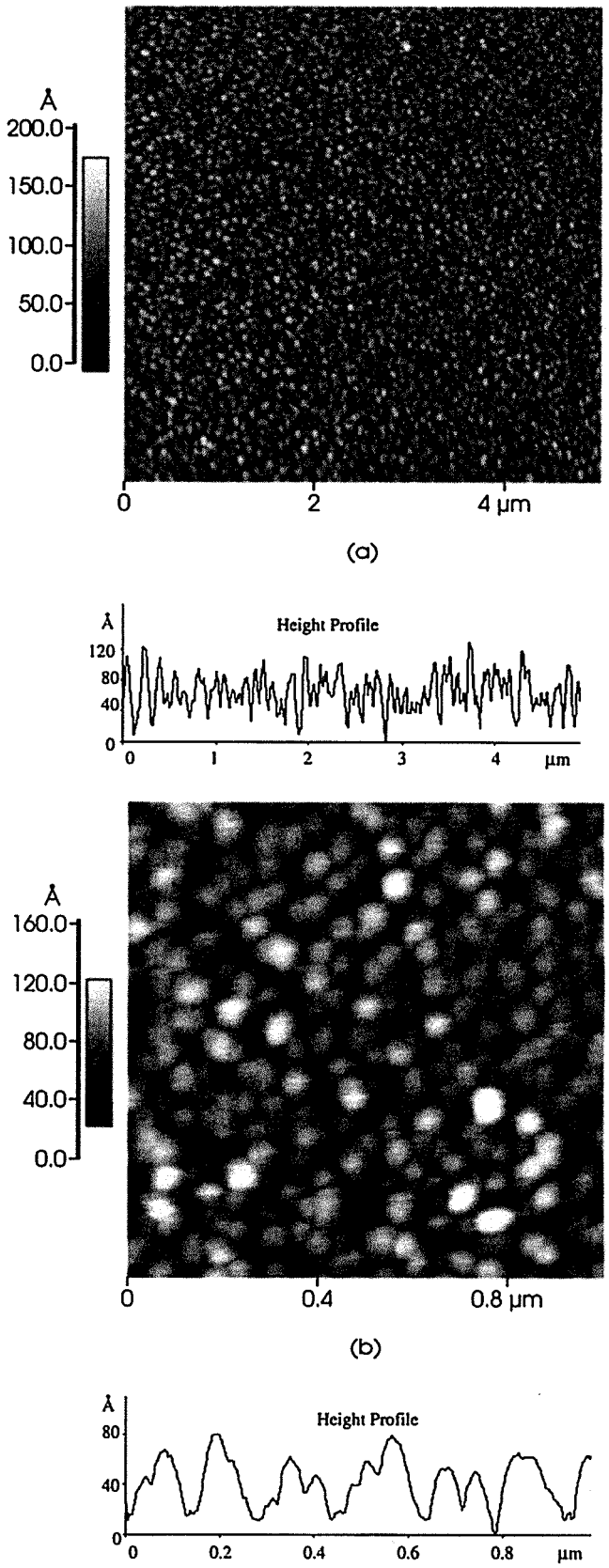

Figure 6. AFM images of (a) PSS/gold−dendrimer nanocomposite bilayer on a silicon wafer and (b) the high-resolution image of the bilayer in part a. The height profiles under the images are typical cross sections along the horizontal direction of the images.

Metal−metal interactions are replaced by polymer−polymer interactions, allowing for greater flexibility in

choosing the deposition and dispersion of metal particles in the final film.

Atomic force microscopy studies of the PSS/Au−dendrimer nanocomposite film can provide the surface morphology and the ordered degree of the nanocomposites in three-dimensional direction. The AFM images of the PSS/Au−dendrimer composite bilayer are shown in Figure 6. The pictures indicate that the films are very uniform with step heights consistent with the size expected for a fifth-generation PAMAM dendrimer. In the AFM images, regular spherical gold−dendrimer nanoclusters (about 70 nm in diameter) can be observed and are uniformly packed on the surface. The result indicates that a strong electrostatic interaction between the multiply charged dendrimer surface and the polyanionic PSS results in the formation of a highly uniform composite film. Lateral dimensions of objects were not well-resolved in AFM because sample preparation, substrate roughness artifacts, and tip effect could also be responsible for the lateral dimensions observed in the AFM.[33] However, the step heights of the objects are well-resolved using this technique and indicate a dendrimer monolayer thickness of roughly 60 Å (see height profiles in Figure 6). The result is approximately consistent with the diameter of 53 Å for spherical G5 PAMAM dendrimers.[20] Gold particle-sized objects were not observed by AFM, which, in addition to the size uniformity of the spherical nanocomposites in contrast with the size distribution of gold particles by TEM (see Figure 4a), provides additional evidence to support incorporation of gold particles into the interior of the dendrimers. AFM morphological observations presented here also show that the Au−dendrimer nanoclusters can be formed into highly uniform multilayers in three-dimensions by electrostatic layer-by-layer deposition. Therefore, electrostatic assembly of dendrimer-encapsulated metal nanoparticles (metal−dendrimer nanocomposite) using oppositely charged polyelectrolytes may be a facile method to fabricate stable and ordered functionalized solid films of nanosized metal.

(33) Ramirez-Aguilar, K. A.; Rowlen, K. L. *Langmuir* **1998**, *14*, 2562.

Conclusion

It is clear from these results that not only can dendrimers be modified with metal clusters within their interiors to give novel nanocomposites but that the surface properties of these dendrimer nanocomposites can be used to fabricate optical-quality thin films using the electrostatic layer-by-layer deposition process. By modifying the dendrimer preparation or the dendrimer/metal combinations used to fabricate films, tunable optical, electronic, and catalyst properties of new nanocomposites will become possible. Incorporation of metal or semiconductor nanoparticles into dendrimers in the form of dendrimer nanocomposites opens up new possibilities for stable, patterned deposition of nanoclusters and offers unprecedented control over layer formation because the surface chemistry, shape, and size of dendrimers used determine the morphology of the fabricated films.

Acknowledgment. Partial financial support from ONR-MURI is gratefully acknowledged. The gold nanocomposite was synthesized at the ARL-MMI Dendrimer Center of Excellence, sponsored by the Army Research Laboratory under Contract DAAL-01-1996-02-0044. L.B. and D.A.T. acknowledge discussions with Drs. Gary Hagnauer (ARL) and Douglas R. Swanson (MMI).

CM990311C